Quaternary International 287 (2013) 63–72

Contents lists available at SciVerse ScienceDirect

Quaternary International

journal homepage: www.elsevier.com/locate/quaint

Changes in Holocene tree cover density in Cabo Frio (Rio de Janeiro, Brazil): Evidence from soil phytolith assemblages

Heloisa H.G. Coe [a,b,c,*], Anne Alexandre [c], Cacilda N. Carvalho [d], Guaciara M. Santos [e], Antonio S. da Silva [f], Leandro O.F. Sousa [g], Igo F. Lepsch [h]

[a] Departamento de Geografia da Faculdade de Professores da UERJ, São Gonçalo, Brazil
[b] Lagemar, UFF, Praia Vermelha, Niterói, RJ, Brazil
[c] CEREGE, CNRS, Aix-Marseille Université, Europôle de l'Arbois, 13545 Aix en Provence, Cedex 04, France
[d] Departamento de Geoquímica, UFF, Centro, Niterói, Brazil
[e] Earth System Science, University of California, Irvine – B321 Croul Hall, Irvine, CA 92697-3100, United States
[f] Instituto de Geografia da UERJ, Rio de Janeiro, Brazil
[g] Departamento de Ciências Vegetais, UFERSA, Mossoró, Brazil
[h] Esalq, USP, Piracicaba, Brazil

ARTICLE INFO

Article history:
Available online 28 February 2012

ABSTRACT

The coastal region of Cabo Frio, in the Brazilian state of Rio de Janeiro, is characterized by xeric vegetation. Surrounded by humid forest, it is considered as a phytogeographical enclave. The vegetation is adapted to the dry conditions which are present locally, mainly due to the Cabo Frio coastal upwelling. Although Quaternary changes in the intensity of the upwelling were reconstructed from coastal lagoons and oceanic sediment records, the lack of continental deposits has precluded vegetation reconstructions. The objective of this study was to investigate the pedogenic features of two soil profiles developed under patches of dry forest in the Cabo Frio area and to assess their potential for inferring past changes in tree cover density, from their phytolith assemblages. For this purpose, field and petrographical observations, C content, C/N ratio, phytolith content and phytolith assemblages were investigated. Soil phytolith assemblages were compared to modern phytolith assemblages. The deepest soil organic carbon (SOC) samples were analyzed in ^{14}C-AMS. Related ^{14}C mean age values were interpreted as the youngest ages of the oldest SOC. These data suggest a first soil development phase, occurring after 13 ka cal BP followed by erosive and depositional episodes and by a second soil development phase. Given the complexity of the studied soil sequences, an attempt to quantify the sources of SOC and phytoliths would require investigation of many more soil samples than the ones collected. This prevents interpretation of the phytolith sequences as continuous chronological sequences. However, for both profiles phytolith indices D/P from A, Ab and bottom horizons can be compared, assuming a bicompartmental distribution of phytoliths in relation with each of the soil development phases. D/P values range from 0.8 to 4, in agreement with what would be expected for dry forest D/P values, and do not substantially change in both profiles. This comparison suggests that the tree cover density of the successive vegetation sources did not suffer considerable change over the period under analysis (last 13 ka for profile A) and never reached the tree density of the humid forest currently widespread in the Rio de Janeiro state.

1. Introduction

The coastal region of Cabo Frio (22°30′–23°00′ S/41°52′–42°42′ W), in the Brazilian state of Rio de Janeiro (Fig. 1), is considered as a phytogeographical enclave (Ab'Saber, 2003). While semi-deciduous forest and rainforest are the natural vegetation dominating the state, xeric formations such as dry forest, xeric shrubland with Cactaceae (also called "*caatinga*") from comparison with the shrubland typical of the semi-arid northeastern part of Brazil (Mooney et al., 1995), restinga shrubland and restinga forest characterize the region of Cabo Frio (Araujo, 1997) (Fig. 2). The Cabo Frio vegetation is adapted to the geomorphic diversity of the area and to the current locally dry conditions, mainly in relation to the Cabo Frio

* Corresponding author. Faculdade de Formaçao de Professores da Universidade do Estado do Rio de Janeiro, Departamento de Geografia. Rua Dr. Francisco Portela, 1470, CEP 24435-005, Sao Gonçalo, Rio de Janeiro, Brazil.
E-mail address: heloisacoe@yahoo.com (H.H.G. Coe).

1040-6182/$ – see front matter © 2012 Elsevier Ltd and INQUA. All rights reserved.
doi:10.1016/j.quaint.2012.02.044

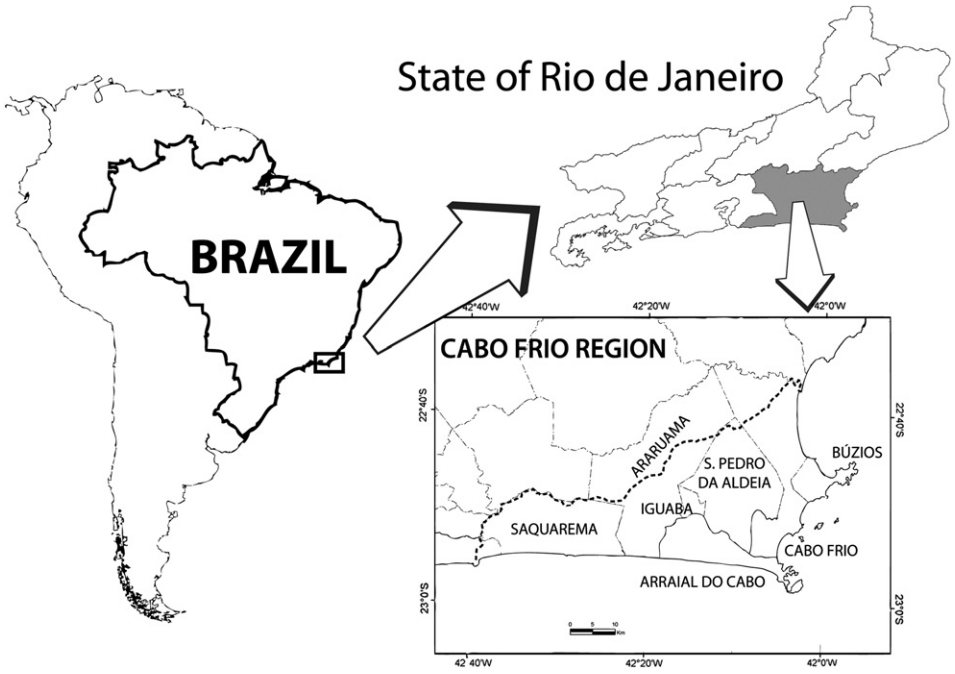

Fig. 1. Location of the Cabo Frio region in the state of Rio de Janeiro, Brazil (modified from Bohrer et al., 2009).

coastal upwelling. Occurrence of upwelling events, concentrated in the austral spring and summer, mainly depend on local and remote northeastern wind regimes favouring upward transportation of the cold thermocline level South Atlantic Central Water towards the coast. The upwelling system leads to a local decrease in precipitation and, hence, to the settlement of a dry microclimate (with a mean annual rainfall of 850 mm), while the regional climate, not affected by the upwelling, is tropical humid (with a mean annual rainfall of 1500 mm) (Barbiere, 1984). Although Quaternary changes in the intensity of the upwelling and in marine transgression/regression phases were reconstructed from coastal lagoons and oceanic sediment records (Ireland, 1987; Barbosa, personal communication; Sylvestre et al., 2005; Laslandes, personal communication; Andrade, personal communication; Oliveira,

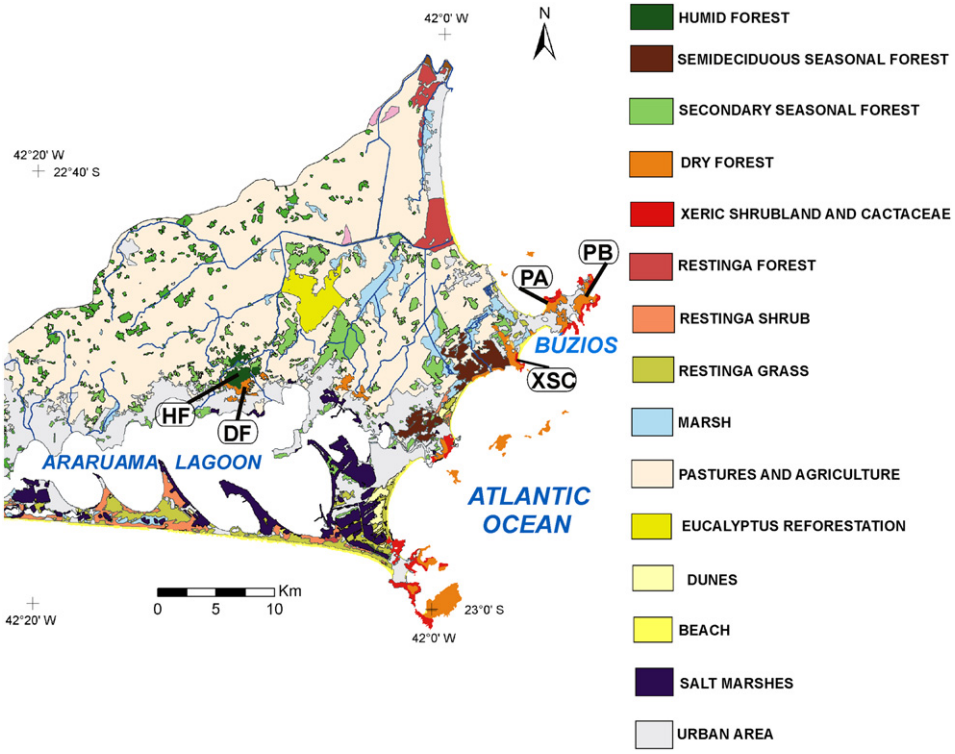

Fig. 2. Vegetation map of the Cabo Frio area (modified from Bohrer et al., 2009). The two investigated soil profiles as well as the sampled sites for modern phytolith assemblages are displayed (white circles). PA: soil profile A; PB: soil profile B; HF: humid forest phytolith assemblage sampling site; DF: dry forest phytolith assemblage sampling site; XSC; xeric shrubland with Cactaceae phytolith assemblage sampling site.

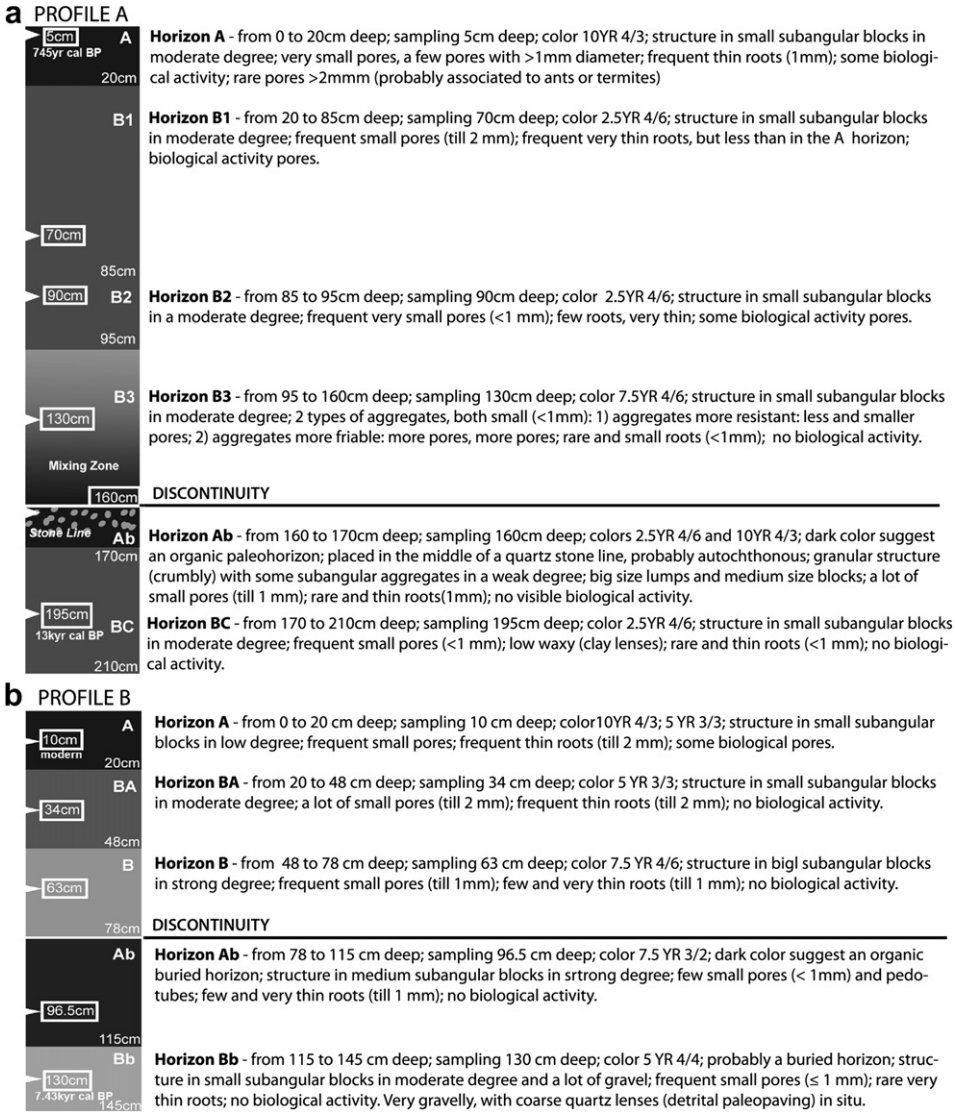

Fig. 3. Schematic description of (a) profile A, showing four main horizons including a buried Ab horizon underlying a discontinuity (in color and structure); (b) profile B, showing five main horizons including a buried Ab horizon underlying a discontinuity (in color and structure). Sampled depths are indicated by white triangles.

personal communication), the lack of continental deposits has precluded vegetation reconstructions. Thus, the history of the Cabo Frio phytogeographical enclave remained unknown. The objective of this study was to investigate the pedogenic features of two soil profiles in the Cabo Frio area and to assess their potential for inferring past changes in vegetation, from their phytolith assemblages. At a given soil depth, phytolith assemblage results from a balance between erosion, deposition, continuous translocation and selective dissolution processes (Alexandre et al., 1999). Analysis of soil phytoliths can provide paleoenvironmental information (e.g. Piperno and Becker, 1996; Blecker et al., 1997; Alexandre et al., 1999) only if those four controls (mentioned above) can be assessed. In the present case, pedological processes were inferred from field observations and petrographical observations. Potential Holocene changes in tree cover density were discussed taking into account pedogenesis, changes with depth in phytolith assemblages, and especially changes in the phytolith index D/P indicative of tree cover density (Alexandre et al., 1997; Bremond et al., 2005a; Barboni et al., 2007). Because soil organic matter (SOM) is composed of a complex mixture of organic molecules of different origins in various stages of decomposition, its bulk ^{14}C analysis can only represent the mean ^{14}C concentration of the soil sample. Mean or apparent ages of SOM from the base of the two soil profiles were estimated based on ^{14}C accelerator mass spectrometry (AMS) analyses. They were assumed to be close to the mean ages of the deepest phytolith assemblages.

2. Regional setting

The Cabo Frio area (Fig. 1) covers 1500 km^2 of a complex geological and geomorphologic setting. Elevation does not exceed 300 m a.s.l. and most of the north–south oriented coastline has been shaped by sea level changes during the Quaternary (Ortega, personal communication). The lithology consists mainly of gneiss, sand and clay materials. Most soils are poorly developed. However, deep weathering profiles with ferruginous concretions and occasional stone-lines can be found on colluvial sandy-clay hills such as in the Buzios peninsula (Muehe, 1994) (Fig. 1). The local climate is tropical dry, with an average annual rainfall of 850 mm, a 4–5 month dry season during austral winter and an average annual temperature of 23 °C (Barbiere, 1984; Duarte, personal communication).

The natural vegetation is composed of a mosaic of forms (Araujo, 1997) comprising (1) tree or shrub "*restinga*" formations,

Table 1
Phytolith concentration, phytolith types, phytolith indices D/P and Bi, SOC concentration and C/N ratio, obtained for the reference samples (DF: dry forest; HF: humid forest; XSC: xeric shrubland with dominance of Cactaceae) and the two soil profiles (PA and PB).

Sample	Horizon depth	Sampling depth	Phytolith amount	Globular Echinate	Globular Granulate	Globular Smooth	Bulliform Cuneiform	Acicular	Bilobate	Cross	Saddle	Elongate	Blocky/ Tabular/ Parallelepiped bulliform	Unclassified Short Cells	Total of Short cells	Unknown	Unclassified phytoliths	Total of phytoliths	Total of counted phytoliths	D/P	Bi	C	C/N
	a	a	b	c	c	c	c	c	c	c	c	c	c	c	c	c	d	d	e			f	
DF				0.19	26.5	3.83	0	3.5	1.15	0.19	2.11	6.33	54.7	1.92	5.4	0.19	29.2	46.52	848	3.0	0	0.89	11.25
HF				0.25	57.3	4.67	0.5	4.2	0.25	0	0.25	4.67	23.8	0.5	1	2.34	33.8	51.72	673	10.1	8.6	0.81	12.75
XSC				34.48	6.5	1.33	2.5	3.4	0.57	0	11.05	7.43	25.6	3.81	15.4	3.04	28.88	41.53	887	0.3	11.6	0.73	9.78
PA A	0–20	5	0.17	1.89	23.5	22.17	0.6	4.2	3.77	0.47	1.89	7.08	31.6	6.60	8.1	14.15	46.72	0.17	602	1.8	4.7	1.73	11.45
PA B1	20–85	65	0.05	1.09	16.1	20.65	2.3	1.9	4.89	0.54	5.43	6.52	37.6	3.26	8.4	26.09	45.89	0.05	756	1.3	18.3		
PA B2	85–95	90	0.19	1.59	23.0	30.16	1.3	4.2	0	0.53	5.29	3.17	27.1	7.41	1.7	16.40	32.67	0.19	486	3.2	18.1	0.83	11.24
PA B3	95–160	130	0.45	3.56	23.9	36.44	1.5	2.7	0	0	2.22	6.22	28.1	0	4.5	12.44	37.11	0.45	706	2.7	17.2	0.87	11.40
PA Ab	160–170	160	0.99	1.14	23.1	14.0	0.5	3.5	0	0.29	0.57	8.57	33.3	1.71	5.8	10	47.85	1	808	2.4	5.1	0.51	13.59
PA BC	170–210	195	0.15	1.09	17.9	9.24	1.6	3.1	0	0	0.54	2.17	55.1	0	0	8.15	29.06	0.16	305	3.8	34.0	0.49	11.04
PB A	0–20	10	0.06	3.51	11.5	4.39	1.8	6.2	1.75	0	0	17.54	28.3	3.51	5.3	9.7	56.4	0.06	308	0.9	13.5	1.91	10.96
PB BA	20–48	34	0.05	6.36	15.0	9.41	1.2	7.2	0	0	0	5.09	43.8	0.25	0.3	6	47.5	0.05	714	1.7	13.8	0.47	9.37
PB B	48–78	63	0.09	6.10	11.7	7.98	0.2	1.9	0.23	0	0.47	6.34	45.6	0.94	2.0	9.3	64.5	0.09	1153	3.0	0	0.79	9.04
PB Ab	78–115	96.5	0.22	0.48	14.6	6.25	1.6	5.7	0.96	0	5.29	9.62	34.4	3.85	10.9	12	47.8	0.22	426	0.8	8.8	0.60	14.25
Pb Bp	115–145	130	0.14	0.97	19.3	14.01	1.4	4.8	0	0	0	2.90	24.1	0.48	0.5	13	57.1	0.14	506	2.9	20.1	0.31	8.34

a: in cm.
b: in % of dry weight <2 mm.
c: in % of the sum of classified phytoliths.
d: in % counted particles.
e: in units.
f: in %.

characterized by medium sized trees and shrubs adapted to dry and nutrient-poor conditions, covering the sandbanks; (2) marshes and lagoon shores covering flooding environments; (3) deciduous dry forest composed of dense trees with thin trunks, 3 to 10 m high, in the colluvial–alluvial plain (Ibraimo et al., 2004); (4) rainforest, also called the *Atlantic low-montana* forest (Rizzini, 1979), in wind-protected or humid sites; (5) xeric shrubland with predominance of Cactaceae (especially the endemic species *Pilosocereus ulei)*, with little floristic diversity but adapted to water stress and disturbance (Araujo, 1997), covering the areas most exposed to sea breezes, like the coastal massifs. Pastures and urban areas are today widespread (Fig. 2).

3. Materials and methods

3.1. Materials

North to the town of Buzios (Fig. 1), two thick soil outcrops located on the gentle slopes of two coastal hills were sampled.

Profile A (22°45′28″S/41°54′28″W) (Fig. 2) is located on the upper part of a 70 m a.s.l. hill covered by a dry forest patch made of Sapindaceae, Ericaceae, Anacardiaceae, Bombacaceae and Euphorbiaceae. Herbaceous Cactaceae, Bromeliaceae and Arecaceae are common. Few Poaceae occur, represented by the Panicoideae subfamilly. However, 200 m away from the sampled soil profile, planted Bambusoideae and invasive Panicoideae are present. This 210 cm depth cambisol (WRB reference soil groups, 2006) is developed at the expense of gneissic rocks. Four main horizons were identified as follows (and presented in detail in Fig. 3a): (1) from 210 to 170 cm, a dark-red clay-sandy BC horizon; (2) from 170 to 160 cm a buried Ab horizon, darker, sandier and with more fine pores than the underlying horizon. A stone line occurs between 165 and 160 cm; (3) at 160 cm a discontinuity is revealed by an abrupt change in color and grain size, leading, from 160 to 20 cm, to a B horizon that can be subdivided as follows: (3a) from 160 to 95 cm depth, a strong brown B3 horizon, more clayey than Ab, presents a structure in small subangular blocks; (3b) from 95 to 85 cm, the occurrence of frequent small pores (<1 mm), of few thin roots and some biopores filled by distinct materials (bioturbation) define a B2 horizon; (3c) from 85 to 20 cm, larger pores, thinner roots and a more clayey texture characterize a B1 horizon. From the base of this B horizon to 140 cm, the presence of aggregates with the color of the underlying Ab horizon evidences a mixing zone; (4) from 20 cm up to the soil surface, an A horizon can be identified from its dark color similar to the color of the Ab horizon, and from many bioturbation features associated with ant or termite activity.

Profile B (22°45′56″S/41°52′47″W) (Fig. 2) is located half way to the top of a 20 m a.s.l. hill covered by a young dry forest. Shrub species are dominated by Ericaceae (predominant), Myrtaceae, Bombacaceae, Clusiaceae and Euphorbiaceae. No Poaceae are present right above the profile, but invasive Panicoideae settle along the road 20 m away. This cambisol was sampled up to 145 cm depth. The gneissic parent rock was not reached. Five main horizons were identified as follows (and presented in detail in Fig. 3b): (1) from 145 to 115 cm, a reddish brown B horizon, very gravelly, presents rare and very thin roots and no biological activity. Coarse quartz lenses suggest a detrital paleopaving; (2) from 115 to 78 cm, a dark brown horizon presents a structure with medium subangular blocks. Few small pores (<1 mm) and pedotubes suggest a buried Ab horizon. Roots are few and thin and no biological activity was identified; (3) A discontinuity in color and structure occurs at 78 cm. From 78 to 48 cm, a lighter and more clayey B horizon presents big subangular blocks, frequent small pores, few and very thin roots and no biological activity; (4) from 48 to 20 cm, a dark reddish brown BA horizon, coarser than the B horizon, presents a structure with small subangular blocks, many small pores, frequent thin roots and no biological activity; (5) from 20 cm to the surface, a dark and very dark reddish brown A horizon presents a structure with small subangular blocks, frequent small pores, thin roots and biopores.

For both profiles, samples were collected at middle depth of each of the observed horizons (Fig. 3).

In order to interpret the soil phytolith assemblages in light of modern phytolith assemblages (Bremond et al., 2005b, 2008), undisturbed soil top samples were collected under three characteristic vegetation types of the Cabo Frio area (Fig. 2): humid forest (HF), dry forest (DF) and xeric shrubland with predominance of Cactaceae (XSC). The sampled humid forest is located at the top of the Serra da Sapiatiba (22°49′05″S/42°09′31″W). It consists of trees of 6–20 m high, belonging to the Arecaceae, Sapindaceae, Rubiaceae and Moraceae families. Epiphytes are abundant. The herbaceous layer is composed of ombrophilous plants, pteridophytes and epiphytic Bromeliaceae. Poaceae and Cyperaceae are absent. The sampled dry forest is located at the base of the Serra da Sapiatiba (22°08′57″S/

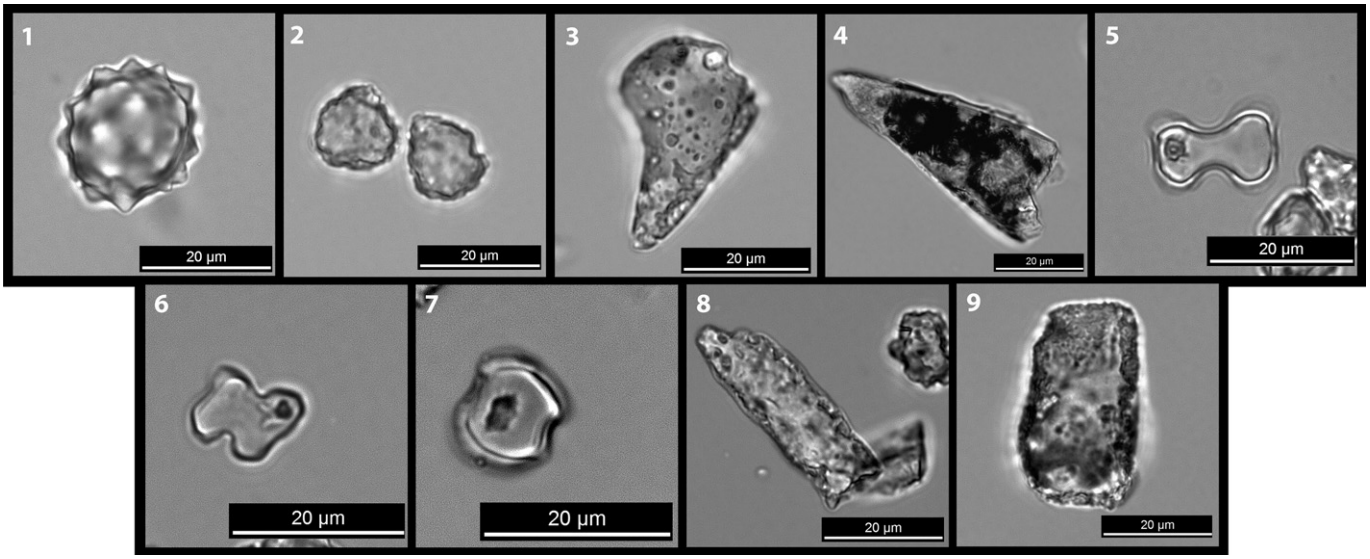

Fig. 4. Main phytolith types observed: (1) Globular echinate, XSC; (2) Globular granulate (DF); (3) Cuneiform bulliform, HF; (4) Acicular, XSC; (5) Bilobate, XSC; (6) Cross, DF; (7) Saddle, XSC; (8) elongate, HF; (9) blocky or parallelepiped bulliform, XSC (Photos Alexandre, 2011).

42°08′57″W). It is dominated by bushes of the Myrtaceae, Euphorbiaceae and Leguminosae families. The herbaceous layer is composed of grasses, mainly Panicoideae, and of some herbaceous dicotyledon (Rubiaceae and Asteraceae families). Some Cactaceae and epiphytic Bromeliaceae are present. The xeric shrubland with predominance of Cactaceae is located close to Tucuns beach, Buzios (22°49′05″S/42°09′31″W). It is dominated by the Cactaceae *Pilosocereus ulei*. Trees from the Anacardiaceae, Apocinaceae, Ericaceae, Bombacaceae, Euphorbiaceae, Clusiaceae and Bignoniaceae families are present. The understory consists of Bromeliaceae, Araceae, Iridaceae and Arecaceae. Poaceae and Cyperaceae are absent. The three sampled sites are located a few meters away from secondary roads or tracks where Panicoideae grasses settle on the edges.

3.2. Methods

3.2.1. Phytolith analysis

3.2.1.1. Chemical extraction and counting. Phytoliths were extracted from 20 g of dry soil, slightly crushed, sieved at 2 mm and processed through the following stages (Kelly, 1990): (1) dissolution of carbonates using HCl (1N); (2) oxidation of organic matter using H_2O_2 (30%) at 90 °C; (3) removal of the clay fraction (<2 μm) by decantation; (4) densimetric separation of opal particles in a heavy liquid of $ZnBr_2$ (density of 2.3 g/cm^3). Particles were dried and weighed after extraction. Phytoliths were then mounted on microscope slides in glycerine for 3D observation and in Canada balsam for counting at 600× magnification. More than 200 phytoliths with a diameter greater than 5 μm and with taxonomic significance were counted.

3.2.1.2. Phytolith types. Phytoliths were classified into ten types following the classification of Twiss (1992); Twiss et al. (1969) improved and completed by phytolith shape descriptions of Mulholland (1989), Fredlund and Tieszen (1994), Kondo et al. (1994), Alexandre et al. (1997); Strömberg (2004), Mercader et al. (2009) and named after the International Code for Phytolith Nomenclature 1.0 (ICPN Working Group, 2005): (1) the Globular echinate type is produced by Palmae (Kondo et al., 1994; Runge, 1999; Runge and Fimbel, 1999; Vrydaghs and Doutrelepont, 2000) but can also be found in Bromeliaceae (Piperno, 1985); (2) the Globular granulate type is produced by tropical trees at low elevation (Scurfield et al., 1974; Kondo et al., 1994; Alexandre et al., 1997; Bremond et al., 2008); (3) the Globular smooth type, appears to have several origins. It has been reported in the epidermis of leaves and in the ray or parenchyma cells of dicot twigs and wood (Kondo et al., 1994); (4) the Cuneiform bulliform cell type is produced in the grass epidermis (Twiss et al., 1969; Kondo et al., 1994) but can also be found in Cyperaceae subject to hydrous stress (e.g. Grigore et al., 2010); (5) the Acicular type from micro-hair and prickles is produced in grass epidermis (Palmer et al., 1985; Kaplan et al., 1992); (6) the Bilobate and (7) Cross short cell types are produced in great quantities by the grass Panicoideae subfamily (Twiss et al., 1969; Mulholland, 1989; Fredlund and Tieszen, 1994; Kondo et al., 1994); (8) the Saddle type is produced in high quantities by the grass Chloridoideae subfamily (Twiss et al., 1969; Mulholland, 1989; Fredlund and Tieszen, 1994; Kondo et al., 1994); (9) the Elongate type originates from the silicified long cells of grass epidermis and (10) the Blocky and Tabular types reported in woody taxa (Strömberg, 2004; Mercader et al., 2009) are not easy to distinguish from the Parallelepiped bulliform types from grasses and were merged in a single morphological group. Phytoliths without taxonomic significance (non-classified phytoliths) because of their original shape, or due to dissolution or fragmentation, were gathered into a non-classified category. Types are presented as

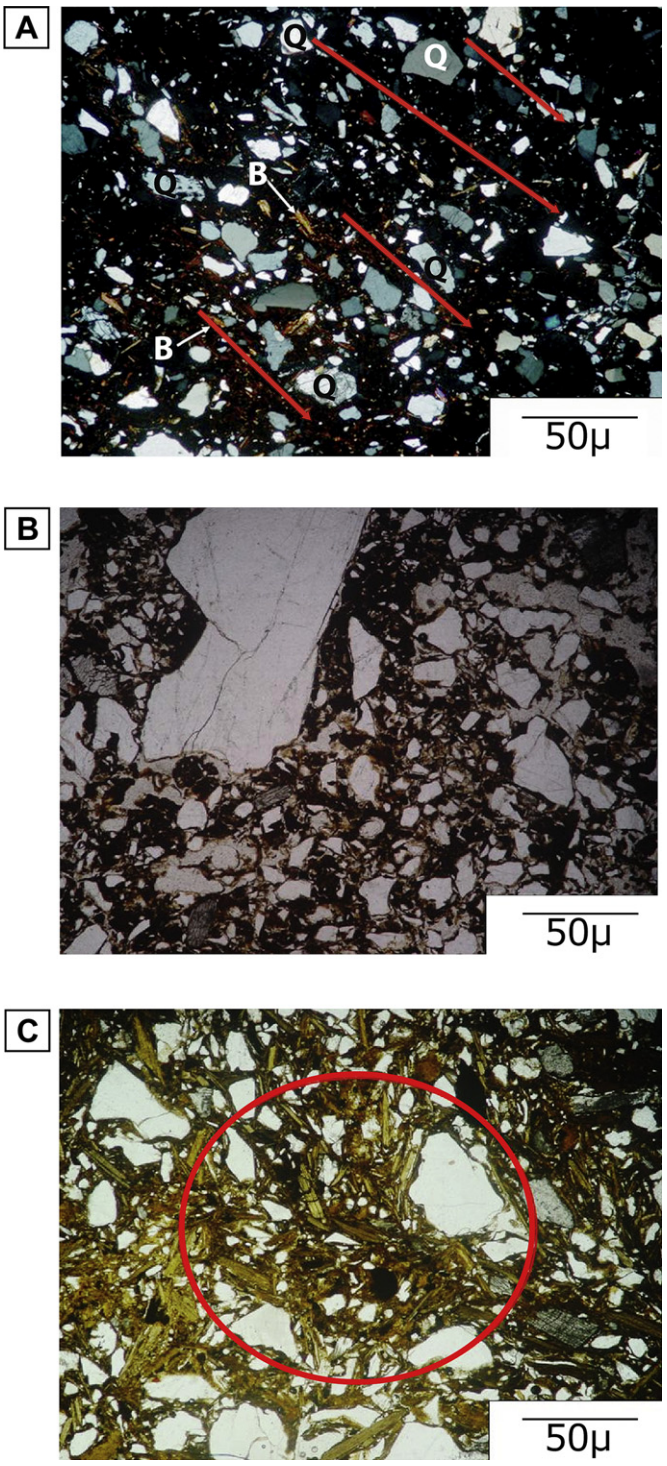

Fig. 5. Petrographical features of B3 and Ab horizons from profile A and of Ab horizon from profile B: (A) profile A B3 horizon above the mixing zone: skeleton, well distributed in the slide, angular to subangular, composed by oriented quartz grains (Q) and weathered biotite grains (B), polarized analyzed light (PAL); (B) profile A Ab horizon: skeleton composed by large (several millimeters) and small quartz grains without any orientation; natural light (NL); (C) profile B Ab horizon: biotite grains with concentric orientation (in red oval) indicate that the origin of this horizon is associated to mass movements (NL). (For interpretation of the references to colour in this figure legend, the reader is referred to the web version of this article.)

percentages of the sum of classified phytoliths. Counting of the same slide by two persons gave reproducibility (SD) of ±2%.

3.2.1.3. Phytolith indices. Two phytolith indices were calculated as follows: (1) the D/P index is the ratio of the dicotyledon phytolith type (Globular granulate) over the sum of Poaceae phytolith types (Short cells + Acicular + Cuneiform bulliform) (Bremond et al., 2005a); (2) The hydrous stress index Bi, previously named Fs (Bremond et al., 2005b; Messager et al., 2010) is the ratio of the Cuneiform bulliform type over the sum of Poaceae phytolith types (Short cells + Acicular + Bulliform cuneiform), expressed as a percentage. Given the low amount of Bilobate type, the aridity index Iph (Fredlund and Tieszen, 1994; Bremond et al., 2005b) was not calculated in this study.

3.2.2. Organic matter analyses

Elemental C and N concentrations were measured with a Carlo Erba elemental analyzer. The limit of detection for C and N was 0.03%. Samples of soil organic carbon (SOC) from the top and the base of the soil profiles (Fig. 3) were selected and processed to undergo ^{14}C-AMS analyses. ^{14}C-AMS analyses were performed at KCCAMS/UCI Facility, Irvine (USA) as following: (a) identifiable components such as plant residues were thoroughly inspected under the microscope and removed; (b) bulk soil samples were then treated with HCl (1N) to remove carbonates; (c) samples were combusted at 900 °C for 3 h in evacuated, flame-sealed quartz tubes together with CuO and silver wire; and (d) the resulting CO_2 was cryogenically clean and subsequently reduced to filaments graphite following an established protocol (Santos et al., 2004). Radiocarbon concentrations are given as fractions of the Modern standard δ^{14}C, and conventional radiocarbon age, following the conventions of Stuiver and Polach (1977). Sample preparation backgrounds were subtracted, based on measurements of ^{14}C-free coal. The accuracy and precision of the AMS measurements performed at the KCCAMS/UCI facility lies in the range of 2–3‰ on modern graphite target samples (Santos et al., 2007). For the interpretation of results, radiocarbon ages were calibrated using CALIB 5.0 program.

3.2.3. Petrographical observations

In order to describe the soil constituents and their arrangement, thin sections of the soil samples were observed under a petrographical microscope and interpreted following Bullock et al. (1985), Delvigne (1998) and Castro (2002).

4. Results

4.1. Modern phytolith assemblages

The three modern phytolith assemblages are presented in Table 1 and Fig. 4. The humid forest assemblage (HF) is dominated by the Globular granulate type (57% of the classified phytoliths).

a

REFERENCE ASSEMBLAGES		D/P	Bi (%)	SOC (% dry weight)	C/N
DF	Dry Forest	3.0	0	0.89	11.25
HF	Humid Forest	10.1	8.6	0.81	12.75
XSC	Xeric Shrub and Cactaceae	0.3	11.6	0.73	9.78

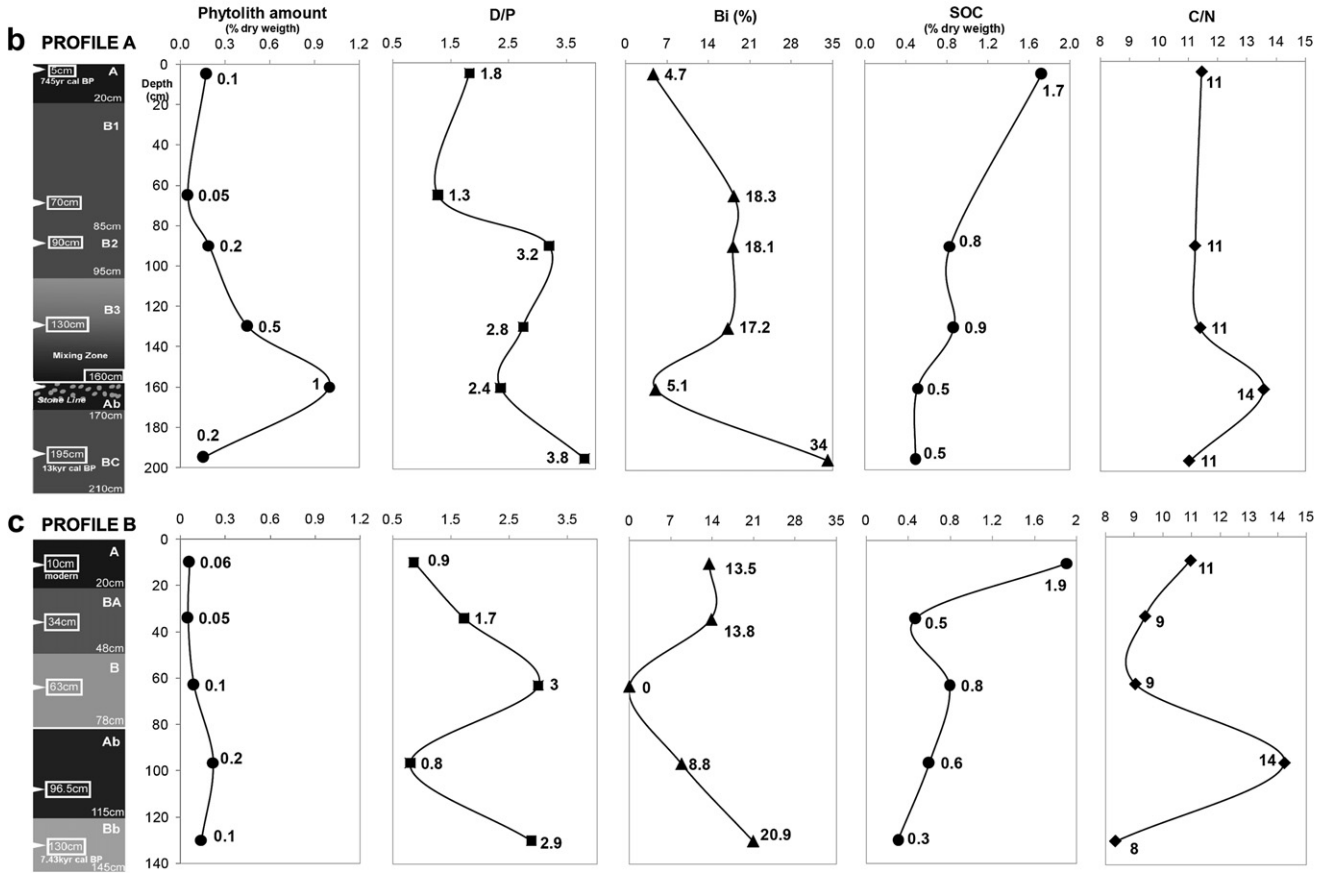

Fig. 6. Phytolith concentration, phytolith indices, C content and C/N values obtained for (a) reference assemblages, (b) soil profile A and (c) soil profile B.

Although neither Poaceae nor Cyperaceae species were observed on the site, some phytolith types produced by grasses are present in small amount: the Elongate and Acicular types both account for more than 4% of the classified phytoliths, and the Short cell types and the Cuneiform Bulliform type do not exceed 1%. Grass phytoliths may originate from the invasive grasses observed on the track's edges close to the site. The dry forest assemblage (DF) show a lower proportion of the Globular granulate type (27%) but a higher proportion of the Short Cell types (5%), in agreement with grass occurrence in the herbaceous layer. The assemblage from the xeric shrubland with predominance of Cactaceae (XSC) is dominated by the Globular Echinate type (34.5%), which can be explained by the presence of Bromeliaceae. Poaceae Short cell types are represented (15%), although no grasses or sedges were found on the site. They may originate from invasive grasses observed on the track's edges close to the site. In spite of the puzzling occurrence of grass phytolith types in HF and XSC assemblages, the D/P index decreases from 10 to 3 and 0.3 respectively for HF, DF and XSC, in agreement with a decrease of the tree cover density.

4.2. Petrographical, C content, C/N and SOC ^{14}C mean age of the soil profiles

Field observations suggested the occurrence of a buried A horizon (Ab) in both profiles, underlying a discontinuity in soil development. Petrographical features supported these observations: Ab horizon from profile A presents a darker color (strong brown) than the overlying (brown) and underlying (red) horizons. Skeleton grains are made of quartz and biotite in both Ab and the overlying B3 horizons. However, although the quartz grains are oriented in B3 above the mixing zone (Fig. 5A), they do not show any orientation in Ab and in the mixing zone (Fig. 5B). While skeleton grains are thin and well sorted in the mixing zone, they are coarser and more angular in the Ab horizon.

In profile B, the Ab horizon is darker (dark brown) than the underlying Bb horizon (reddish brown) and contains feldspar, quartz and weathered biotite grains (Fig. 5C). The biotites are deformed, incurved and have concentric orientation, suggesting that this material is colluvial, originating from a catastrophic mass movement. In the basement rocks, biotite are oriented horizontally due to the intense process of metamorphism occurred at the site (Schmitt, personal communication). Thus, the way as biotites are organized on Ab horizon indicates the occurrence of transport processes, whether through erosion or mass movements, probably the latter, considering the semi-arid trend of the local climate.

For both profiles, SOC content values decrease drastically with depth in the first tenths of a cm and more slowly below, with, however, a slight increase in the B horizons developed above the discontinuities (Fig. 6). C/N values clearly stabilize around 11 and 9 for profile A and B respectively, except at depth 170–160 cm (Ab horizon from profile A) and 115–78 cm (Ab horizon from profile B) where C/N reaches 14, in agreement with field and petrographical evidence of buried Ab horizons (Fig. 6). A decreasing logarithmic trend in SOC is common to tropical and temperate soils in equilibrium with their litter input and controlled by particle translocation and mineralization. It can be modelled as a bicompartimental distribution assuming two pools of SOC (Jenkinson and Ravner, 1977; O'Brien and Stout, 1978; Balesdent and Guillet, 1982; Parton et al., 1987; Alexandre et al., 1997, 1999). One pool is recycled rapidly and is in dynamic equilibrium. The input for that pool is litter at the top of the profile. With time, the organic matter in that pool is translocated downward and is mineralized, decreasing to trace levels at the bottom of the profile. The second pool is more stable and its translocation leads to a constant content with depth. At the base of the soil development, nearly all of the SOC is in the stable pool.

In regard to the studied soil profiles, although petrographical features suggest that the soils experienced several developments interrupted by an erosion phase, the deepest SOC is assumed to mainly belong to the oldest stable pool. Its ^{14}C mean age value can thus be interpreted as the youngest age of the oldest SOC of a soil. For profiles A and B, they are respectively ^{14}C 11,175 $\pm$ 25 yrs/13.0 ka cal BP (#UCIG21168) and ^{14}C 6535 $\pm$ 15 yrs/7.4 ka cal BP (#UCIG21107). ^{14}C mean age value of the top SOC is ^{14}C 700 $\pm$ 15 yrs/745 yr cal BP (#UCIG21163) for profile A and post-bomb or modern (#UCIG21104) for profile B.

4.3. Phytolith amount, assemblages and indices from the soil profiles

4.3.1. Profile A

In the A horizon, the D/P index (1.8) is close to the one obtained for the DF modern assemblage (3), in agreement with the effective settlement of a dry forest patch on the slope (Table 1, Figs. 4 and 6). The Bi index is higher (4.7 *vs* 0%). Along the soil profile, phytolith concentration stabilizes between 0.05 and 0.2% dry weight except in the buried humic horizon (1% dry weight) and right above, in the mixing horizon (0.5% dry weight). The D/P index ranges between 1.3 and 3.8, far below the HF value (10) and published values previously obtained from humid forest sites (Alexandre et al., 1997; Barboni et al., 1999). The Bi index clearly increases with depth from 4.7 to 34% (excepted in the buried horizon), in relation to a decrease in grass short cell phytoliths below 90 cm in depth.

4.3.2. Profile B

In the humic horizon, the D/P index (0.8) is lower than the one found for DF and from the A horizon of profile A (Table 1, Figs. 4 and 6), in agreement with the current settlement of a drier and younger dry forest above profile. Bi (13.5%) is close to the one obtained for XCS. Along the soil profile, phytolith concentration is stable, ranging between 0.1 and 0.2% dry weight. The D/P index stays low, ranging from 0.8 to 2.9. The Bi index varies a lot, ranging from 0 to 20.9% without any intelligible pattern.

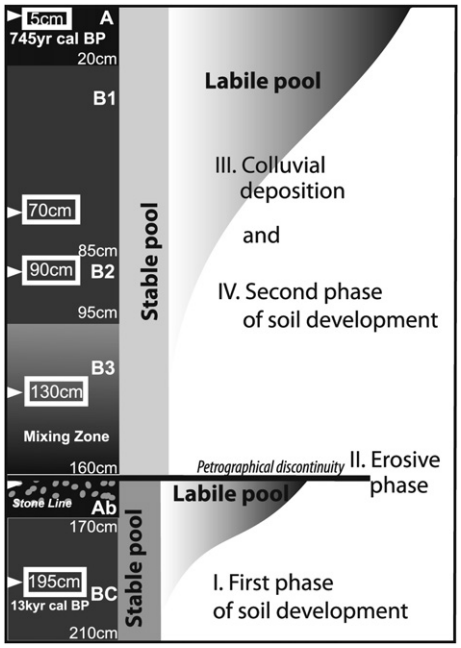

Fig. 7. Profile A: schematic representation of two phases of soil development and bicompartmental distribution of phytoliths in relation with those two phases.

5. Discussion and conclusion

5.1. Steps in soils development

Accumulation and erosion processes acting on soil should be considered in order to establish a balance between contributions and losses of material (including phytoliths). These processes depend on the topographic position of the profile, soil type, vegetation cover and rainfall patterns that can lead to erosion and colluvial deposition from the upward weathering mantle (Piperno and Becker, 1996). In the present study, field and petrographical observations, as well as C/N and phytolith concentration values suggest the occurrence, for both soil profiles, of a first phase of soil development, indicated by the occurrence of a buried humic horizon in both soil profiles, followed by an erosive phase, again in both profiles, materialized by a petrographical discontinuity. A third phase of colluvial deposition led to the burial of the humic horizons (Ab). From there a second soil development started leading to the formation of the A and B horizons in equilibrium with the current vegetation (Fig. 7).

5.2. Clues on the Holocene evolution of the vegetation at Cabo Frio

The two phytolith sequences thus experienced erosion and deposition phases superimposed on translocation/dissolution processes common to soil particles. At depth, below the discontinuities, phytolith assemblages originated from three sources that were 1) and 2) the mean vegetations developed during the two successive soil developments, plus 3) the mean vegetation developed upward before the erosion/deposition phase, in between the two soil developments (Fig. 7). Given the complexity of the studied soil sequences, attempt to quantify the sources of SOC and phytoliths would require investigation of many more soil samples than the ones collected. This prevents interpreting the phytolith sequences as continuous chronological sequences. However, for both profiles, radiocarbon mean ages of the oldest and youngest SOC help to roughly constrain the time frame recorded by the phytolith sequences. Additionally, comparison of phytolith assemblages from A, Ab, and bottom horizons gives several clues about the evolution of the vegetation in Cabo Frio.

^{14}C mean age of the oldest SOC from profile A is 13.0 ka cal BP, and top SOC ^{14}C age is 745 yr cal BP. Several studies suggested that phytolith and organic compounds from tropical soils show close translocation rates (Piperno and Becker, 1996; Alexandre et al., 1999). Thus the assumption is made that most of the phytoliths distributed in soil profile A are younger than 13 ka cal BP (Fig. 7). Sampling of profile B did not reach the parent rocks. SOC ^{14}C age of 7.4 ka cal BP obtained for the Bb horizon results from a mixing between stable old SOC and decreasing younger SOC. The oldest SOC from profile B is thus older than 7.4 ka cal BP. In both soil profiles, the buried Ab horizon is characterized by a relatively high concentration in phytoliths. At these depths, phytolith assemblages should mainly originate from the vegetation in equilibrium with the first phase of soil development (Fig. 7). Associated D/P indices are close to the D/P values found for the current A horizons (1.8 *vs* 2.4 for profile A, 0.9 *vs* 0.8 for profile B) suggesting that prior to the erosion/deposition phases the vegetation was close to the modern one. The bottom of both profiles should be dominated by old and stable phytoliths translocated from the Ab horizons (Fig. 7). Both show D/P values slightly higher but still close to that obtained for the Ab and A horizons.

In the literature, D/P values ranging from 0.2 to 1 are obtained for vegetation woodier than grasslands but less woody than dry forests (Bremond et al., 2005b; Barboni et al., 2007), while D/P values close or higher than 10 are found for rainforests (Alexandre et al., 1997, submitted). D/P values obtained for reference phytolith assemblage DF, and for A horizons of profiles A and B (respectively 3, 1.8 and 0.9), all covered by dry forests, are thus in the lower part of the range between those two groups. D/P values obtained for Ab and bottom horizons of profiles A and B ($>$0.8 and $<$4) are also in the lower part of the range between those two groups. Although assessment of the accuracy of D/P from 1 to 10 for quantifying with precision relative changes in tree cover density is still to be done, these results suggests the following: 1) the tree cover density of the successive vegetation sources was close to the ones found for modern dry forests in the area; 2) the tree cover density did not significantly change over the considered time period (last 13 ka for profile A) and 3) the tree cover density never reached the one found in humid forest currently widespread in the Rio de Janeiro state.

Acknowledgements

This work was supported, in France, by a CAPES PhD grant and, in Brazil, by a FAPERJ grant. Authors are especially grateful to Prof. Daniel Vidal and all staff of EMBRAPA for supporting the phytolith extractions. We also express special thanks to Prof. Marcelo Bernardes, from Universidade Federal Fluminense, for helpful discussions about organic analysis and to Cintia Ventania and Maria Fernanda Alvarez for the edition of the figures. We also thank two anonymous reviewers for their very constructive reviews.

References

Ab'Saber, A.N., 2003. Redutos de cactáceas, jardins da natureza. Scientific American Brasil 19.

Alexandre, A., Meunier, J.-D., Lezine, A.-M., Vincens, A., Schwartz, D., 1997. Phytoliths: indicators of grassland dynamics during the late Holocene in intertropical Africa. Palaeogeography, Palaeoclimatology, Palaeoecology 136, 213–229.

Alexandre, A., Meunier, J.-D., Mariotti, A., Soubies, F., 1999. Late Holocene Phytolith and carbon-isotope record from a Latosol at Salitre, South-Central Brazil. Quaternary Research 51, 187–194.

Araujo, D.S.D., 1997. Cabo Frio region. In: Davis, S.D., Heywood, V.H., Herrera-MacBryde, O., Villa-Lobos, J., Hamilton, A.C. (Eds.), Centers of Plant Diversity: A Guide and Strategy for Their Conservation: The Americas. WWF/IUCN, Oxford, pp. 373–375.

Barbiere, E.B., 1984. Cabo Frio e Iguaba Grande, dois microclimas distintos a um curto intervalo espacial. In: Restingas: Origem, Estrutura, Processos. CEUFF, Niterói, pp. 3–13.

Barboni, D., Bremond, L., Bonnefille, R., 2007. Comparative study of modern phytolith assemblages from inter-tropical Africa. Palaeogeography, Palaeoclimatology, Palaeoecology 246, 454–470.

Barboni, D., Bonnefille, R., Alexandre, A., Meunier, J.D., 1999. Phytoliths as paleoenvironmental indicators, West Side Middle Awash Valley, Ethiopia. Palaeogeography, Palaeoclimatology, Palaeoecology 152, 87–100.

Balesdent, J., Guillet, B., 1982. Les datations par le ^{14}C des matières organiques des sols. Contribution a l'étude de l'humification et du renouvellement des substances humiques. Sciences du sol 2, 93–112.

Blecker, S.W., Yonker, C.M., Olson, C.G., Kelly, E.F., 1997. Paleopedologic and geomorphic evidence for Holocene climate variation, Shortgrass Steppe, Colorado, USA. Geoderma 76, 113–130.

Bohrer, C.B.A., Dantas, H.G.R., Cronemberger, F.M., Vicens, R.S., Andrade, S.F., 2009. Mapeamento da Vegetação e do Uso do Solo no Centro de Diversidade Vegetal de Cabo Frio, Rio de Janeiro, Brasil. Rodriguésia 60, 1–23.

Bremond, L., Alexandre, A., Hély, C., Guiot, J., 2005a. A phytolith index as a proxy of tree cover density in tropical areas: calibration with Leaf Area Index along a forest-savanna transect in southeastern Cameroon. Global and Planetary Change 45, 277–293.

Bremond, L., Alexandre, A., Peyron, O., Guiot, J., 2005b. Grass water stress estimated from phytoliths in West Africa. Journal of Biogeography 32, 311–327.

Bremond, L., Alexandre, A., Wooler, M.-J., Hély, C., Willianson, D., Schaëffer, P., Majule, A., Guiot, J., 2008. Phytolith indices as proxies of grass subfamilies on East African tropical mountains. Global and Planetary Change 61, 209–224.

Bullock, P., Fedoroff, N., Jongerius, A., Stoops, G., Tursina, T., 1985. Handbook for Soil Thin Section Description. Waine Research Publs. 152 p.

Castro, S.S., 2002. Micromorfologia de solo – base para descrição de lâminas delgadas. In: Apostila da disciplina Micromorfologia de Solos. UFG/UNICAMP, Goiânia/Campinas. Impresso e CD-ROM. 135 p.

Delvigne, J.E., 1998. Atlas of Micromorphology of Mineral Alteration and Weathering. In: The Canadian Mineralogist Special Publication 3/ORSTOM éditions. 494 p.

Fredlund, G., Tieszen, L.L., 1994. Modern phytolith assemblages from the North American Great Plains. Journal of Biogeography 21, 321–335.
Grigore, M.N., Toma, C., Boscaiu, M., 2010. Ecological implications of bulliform cells on halophytes, in salt and water stress natural conditions. Analele stiinþifice ale Universitãþii "Al. I. Cuza" Iasi LVI. 5–15.
Ibraimo, M.M., Schaefer, C.E.G.R., Ker, J.C., Lani, J.L., Rolim-Neto, F.C., Albuquerque, M.A., Miranda, V.J., 2004. Gênese e Micromorfologia de Solos sob Vegetação Xeromórfica (caatinga) na Região dos Lagos (RJ). Rev. Bras. Ciên. Solo 28, 695–712.
ICPN Working Group, Madella, M., Alexandre, A., Ball, T., 2005. International code for phytolith nomenclature 1.0. Annals of Botany 96, 253–260.
Ireland, S., 1987. The Holocene sedimentary history of coastal lagoons of Rio de Janeiro state, Brazil. In: Tooley, M., Shennan, I. (Eds.), Sea-Level Changes. Basil Blackwell Ltd., Oxford, pp. 25–66.
Jenkinson, D.J., Ravner, J.H., 1977. The turnover of soil organic matter in some of the Rothamsted classical experiments. Soil Science 123, 298–305.
Kaplan, L., Smith, M.B., Sneddon, L.A., 1992. Cereal grain phytoliths of Southwest Asia and Europe. Phytoliths systematics, emerging issues. In: Rapp, G.J., Mulholland, S.C. (Eds.). Advances in Archaeological and Museum Science, New York, pp. 149–174.
Kelly, E.F., 1990. Method for Extracting Opal Phytoliths from Soil and Plant Material. Intern. Rep., Dep. Agron. Colorado State University, Fort Collins.
Kondo, R., Childs, C., Atkinson, I., 1994. In: L.C.N. Zealand (Ed.), Opal Phytoliths of New Zealand. Manaaki Whenua Press. 85 p.
Mercader, J., Bennett, T., Esselmont, C., Simpson, S., Walde, D., 2009. Phytoliths in woody plants from the Miombo woodlands of Mozambique. Annals of Botany 104, 91–113.
Messager, E., Lebreton, V., Marquer, L., Russo-Ermolli, E., Orain, R., Renault-Miskovsky, J., Lordkipanidze, D., Despriée, J., Peretto, C., Arzarello, M., 2010. Palaeoenvironments of early hominins in temperate and Mediterranean Eurasia: new palaeobotanical data from Palaeolithic key-sites and synchronous natural sequences. Quaternary Science Reviews, 1–9.
Mooney, H.A., Bullock, S.H., Medina, E., 1995. Seasonally dry tropical forests. Introduction. In: Bullock, S.H., Mooney, H.A., Medina, E. (Eds.), Seasonally Dry Tropical Forests, pp. 1–8.
Muehe, D., 1994. Lagoa de Araruama: geomorfologia e sedimentação. Cadernos Geociência IBGE 10, 53–62.
Mulholland, S.C., 1989. Phytoliths shape frequencies in North Dakota grasses: a comparison to general patterns. Journal of Archaeological Science, 489–511.
O'Brien, B.J., Stout, J.D., 1978. Movment and turnover of soil organic matter as indicated by carbon isotope measurements. Soil Biology Biochemistry 10, 309–317.
Palmer, P.G., Gerbeth-Jones, S., Hutchison, S., 1985. A scanning electron microscope survey of the epidermis of East African grasses, III. Smithsonian Contribution to Botany 55, 135.
Parton, W.J., Schimel, D.S., Cole, C.V., Ojima, D.S., 1987. Analysis of factors controlling soil organic matter levels in Great Plains grasslands. Soil Science Society of America Journal 51, 1173–1179.
Piperno, D.R., 1985. Phytolith analysis and tropical paleo-ecology: production and taxonomic significance of siliceous forms in new world plant domesticates and wild species. Review of Palaeobotany and Palynology 45, 185–228.
Piperno, D.R., Becker, P., 1996. Vegetacional history of a site in the Central Amazon Basin Derived from phytolith and charcoal records from natural soils. Quaternary Research 45, 202–209.
Rizzini, C.T., 1979. Tratado de Fitogeografia do Brasil. EDUSP, São Paulo.
Runge, F., 1999. The opal phytolith inventory of soils in central Africa - quantities, shapes, classification, and spectra. Review of Palaeobotany and Palynology 107, 23–53.
Runge, F., Fimbel, R., 1999. Opal phytoliths as evidence for the formation of savanna islands in the rain forest of Southeast Cameroon. In: Heine, K., Runge, G.E.J. (Eds.), VXth INQUA Conference (15th: 1999: Durban South Africa) – Palaeoecology of Africa and the Surrounding Islands. International Union for Quaternary Research, Tokyo, pp. 171–189.
Santos, G.M., Southon, J.R., Druffel-Rodriguez, K.C., Griffin, S., Mazon, M., 2004. Magnesium perchlorate as an alternative water trap in AMS graphite sample preparation: a report on sample preparation at the KCCAMS facility at the University of California. Irvine. Radiocarbon 46, 165–173.
Santos, G.M., Moore, R.B., Southon, J.R., Griffin, S., Hinger, E., Zhang, D., 2007. AMS ^{14}C sample preparation at the KCCAMS/UCI facility: status report and performance of small samples. Radiocarbon 49, 255–269.
Scurfield, G., Anderson, C.A., Segnit, E.R., 1974. Silica in woody stems. Australian Journal of Botany 22, 211–229.
Strömberg, C.A.E., 2004. Using phytolith assemblages to reconstruct the origin and spread of grass-dominated habitats in the great plains of North America during the late Eocene to early Miocene. Palaeogeography, Palaeoclimatology, Palaeoecology 207, 239–275.
Stuiver, M., Polach, H., 1977. Discussion: reporting of ^{14}C data. Radiocarbon 19 (3), 355–363.
Sylvestre, F., Sifeddine, A., Turcq, B., Gil, I.M., Albuquerque, A.L.S., Lallier-Vergès, E., Abrão, J., 2005. Hidrological changes related to the variability of the tropical South American climate from the Cabo Frio lagoonal system (Brazil) during the last 5000 years. The Holocene 15, 625–630.
Twiss, P.C., 1992. Predicted world distribution of C3 and C4 grass phytoliths. In: Mulholland, S.C. (Ed.), Phytoliths Systematics: Emerging Issues. Advance Archaeological Museum Science, vol. 1. Plenum Press, New York, pp. 113–128.
Twiss, P.C., Suess, E., Smith, R.M., 1969. Morphological classification of grass phytoliths. In: Procedure of Soil Sci. Soc. Am, pp. 109–115.
Vrydaghs, L., Doutrelepont, H., 2000. Analyses phytolithariennes: acquis et perspectives. In: Servant-Vildary, S., Servant, M. (Eds.), Dynamiques à long terme des écosystèmes forestiers intertropicaux. UNESCO, Paris.